International Journal of Automotive Technology, Vol. 8, No. 2, pp. 137–147 (2007)

1229-9138/2007/033-02

ANALYSIS OF HCCI COMBUSTION CHARACTERISTICS BASED ON EXPERIMENTATION AND SIMULATIONS–INFLUENCE OF FUEL OCTANE NUMBER AND INTERNAL EGR ON COMBUSTION

A. IIJIMA[1)*], K. YOSHIDA[1)], H. SHOJI[1)] and J. T. LEE[2)]

[1)]Department of Mechanical Engineering, College of Science and Technology, Nihon University, 1-8-14 Kanda-Surugadai, Chiyoda-ku, Tokyo 101-8308, Japan
[2)]School of Mechanical Engineering, Sungkyunkwan University, Gyeonggi 440-746, Korea

(Received 7 August 2006; Revised 2 December 2006)

ABSTRACT–Homogenous Charge Compression Ignition (HCCI) combustion systems can be broadly divided for the process applied to 4-stroke and 2-stroke engines. The former process is often referred to as simply HCCI combustion and the latter process as Active Thermo-Atmosphere Combustion (ATAC). The region of stable engine operation tends to differ greatly between the two processes. In this study, it was shown that the HCCI combustion process of a 4-stroke engine, characterized by the occurrence of autoignition under a high compression ratio, a lean mixture and wide open throttle operation, could be simulated by operating a 2-stroke engine at a higher compression ratio. On that basis, a comparison was made of the combustion characteristics of high-compression-ratio HCCI combustion and ATAC, characterized as autoignited combustion in the presence of a large quantity of residual gas at a low compression ratio and part throttle. The results showed that one major difference between these two combustion processes was their different degrees of susceptibility to the occurrence of cool flame reactions. Compared with high-compression-ratio HCCI combustion, the ignition timing of ATAC tended not to change in relation to different fuel octane numbers. Furthermore, when internal EGR was applied to high-compression-ratio HCCI combustion, it resulted in combustion characteristics resembling ATAC. Specifically, as the internal EGR rate was increased, the ignition timing showed less change in relation to changes in the octane number and the region of stable engine operation also approached that of ATAC.

KEY WORDS : Internal combustion engine, Combustion, Ignition, HCCI, ATAC, Internal EGR

NOMENCLATURE

ε : effective compression ratio [–]
ϕ : intake equivalence ratio [–]
η_s : scavenging efficiency [–]
γ : residual gas ratio [–]
θ : crank angle [deg.]
θ_{on} : ignition timing [deg.]
θ_{peak} : time of hot flame peak [deg.]
HRR : heat release rate [J/deg.]
SR : scavenging ratio [–]
N : engine speed [rpm]
P : in-cylinder pressure [MPa]
Q_{Hmax} : maximum hot flame value [J/deg.]
RON : research octane number
WOT : wide open throttle
T_{epc} : temperature at the exhaust port closing [K]
T_{ex} : exhaust gas temperature [K]
T_{sc} : scavenging temperature [K]
T_r : residual gas temperature [K]
T_g : mean gas temperature

*Corresponding author. e-mail: iijima@mech.cst.nihon-u.ac.jp

1. INTRODUCTION

Further improvement of the efficiency of internal combustion engines (i.e., reduction of specific fuel consumption) and the attainment of cleaner exhaust emissions are required today in order to make effective use of energy resources and preserve the global environment. Methods of improving the thermal efficiency of gasoline engines include raising the compression ratio to an optimum level of around 14:1–16:1, adopting lean-burn combustion to improve the specific heat ratio and reduce heat losses, and reducing pumping work. Diesel engines already attain high thermal efficiency, but the difficulty of simultaneously reducing their nitrogen oxide (NOx) and soot levels remains a major issue to be addressed.

Against this backdrop, the Homogeneous Charge Compression Ignition (HCCI) (Thring, 1989) engine has attracted much interest because it achieves clean combustion

with an ultra-low NOx level and no soot emission when operated under a non-throttled, lean-burn condition at an optimized compression ratio (Lee *et al.*, 2004; Choi *et al.*, 2004; Sato *et al.*, 2006).

HCCI combustion processes can be broadly divided between the systems used in 2-stroke engines and those applied to 4-stroke engines. The former type is known by different names such as Active Thermo-Atmosphere Combustion (ATAC) (Onishi *et al.*, 1979) or Activated Radicals (AR) combustion (Ishibashi *et al.*, 1994) and is characterized by the application of a large quantity of residual gas (internal exhaust gas recirculation) to induce autoignition. The latter type is often referred to as simply HCCI combustion. Other designations that are sometimes applied to the combustion process include Premixed Charge Compression Ignition (PCCI) (Aoyama *et al.*, 1996) and Controlled Auto Ignition (CAI) (Lavy *et al.*, 2000).

Table 1 gives a relative comparison of the engine operating parameters in the case of ATAC in 2-stroke engines and HCCI combustion in 4-stroke engines. It is clear that there are many differences between the two processes. The HCCI combustion process is being widely researched in 4-stroke engines at present, but even in this case, attempts are being made to expand the operation region by applying internal EGR (Urushihara *et al.*, 2003), which is a characteristic of ATAC. There is a tendency for the features of the 2-stroke HCCI combustion process to be incorporated in the 4-stroke variety.

In this study, it was demonstrated that HCCI combustion in a 4-stroke engine could be simulated by operating a 2-stroke engine at a higher compression ratio. On that basis, a comparison was made with the characteristics of HCCI combustion in a 2-stroke engine under ordinary operating conditions (which will be referred to here as ATAC). Combustion characteristics were then investigated when internal EGR was applied under HCCI conditions.

The engine operating conditions used in the experiments are shown in Figure 1. The horizontal axis indicates the scavenging ratio and the vertical axis shows the effective compression ratio. Three sets of operating conditions, summarized below as (1) to (3), were created by using different compression ratios and throttle openings

Table 1. Relative comparison of the engine operating characteristics for ATAC in 2-stroke engines and HCCI combustion in 4-stroke engines.

	2-stroke HCCI (ATAC)	4-stroke HCCI
Compression ratio	Low	High
Engine speed	High	Low
Throttle opening	Part throttle	WOT

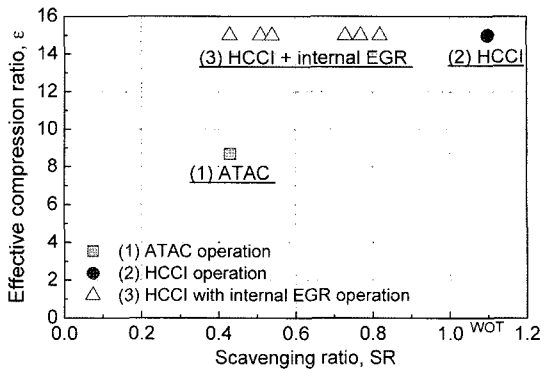

Figure 1. Map of operating conditions for ATAC, HCCI and HCCI with internal EGR.

and with/without internal EGR. An analysis was made of the combustion characteristics obtained under each set of conditions.

(1) ATAC: autoignited combustion achieved with a compression ratio of 8.7:1 and part throttle, and corresponding to conventional HCCI combustion in a 2-stroke engine.
(2) HCCI combustion: HCCI combustion simulating that in a 4-stroke engine and achieved with a high compression ratio (ε=15:1), WOT and a lean mixture.
(3) HCCI combustion with internal EGR: combustion under the HCCI conditions (ε=15:1) and with the application of internal EGR that is characteristic of ATAC.

2. EXPERIMENT AND CALCULATION

2.1. Experimental Equipment and Procedure

The specifications of the 2-stroke, air-cooled, single-cylinder test engine used in this study are given in Table 2. The compression ratio of the engine was varied by changing the clearance volume of the cylinder head. Primary reference fuels (PRF), consisting of different blends of iso-octane and n-heptane, and regular gasoline were used as the test fuels. The configuration of the test equipment used is shown in Figure 2. A crystal pressure

Table 2. Specifications of test engine.

2-stroke air cooled SI engine	
Scavenging type	Schnürle
Bore × Stroke	72 × 60 mm
Displacement	244 cm^3
Effective compression ratio	8.7:1 (ATAC) 15:1 (HCCI)
Test fuels	PRF (0-100 RON) Gasoline (91 RON)

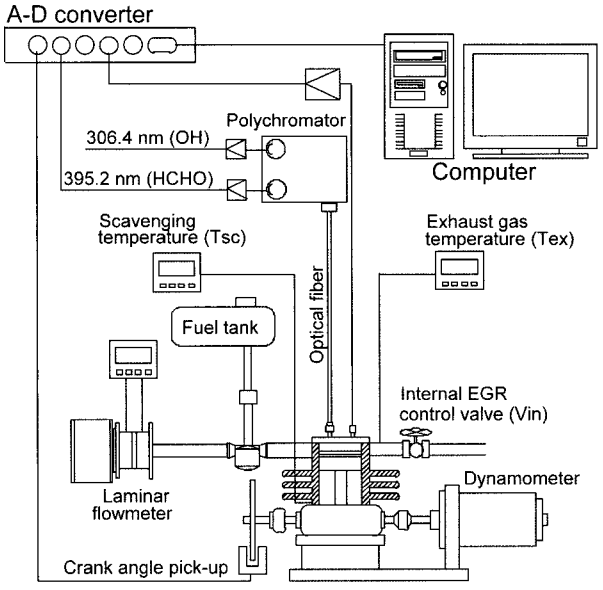

Figure 2. Configuration of test equipment.

transducer was installed in the top of the cylinder head to measure the cylinder pressure (P). The light emission spectra of combustion flame radicals in the combustion chamber were measured in order to analyze autoignition behavior. Light from the combustion flame was extracted through a quartz observation window provided in the top of the cylinder head and transmitted via an optical fiber cable, having core diameter of 1 mm, into a polychromator (Shoji *et al.*, 1998). It was then separated into two wavelengths of 395.2 nm, corresponding to formaldehyde (HCHO), and 306.4 nm, corresponding to the OH radical. The light at each wavelength was converted to an electric signal by a photomultiplier and measured. The two measured wavelengths served the following respective purposes (Gaydon, 1957).

395.2 nm (HCHO): distinctive light emission spectrum corresponding to cool flame reactions that occur prior to ignition

306.4 nm (OH radical): light emission spectrum of the OH radical that plays an important role in the progress of combustion reactions

In addition, K-type thermocouples were used to measure the scavenging temperature (T_{sc}) and exhaust temperature (T_{ex}) in order to monitor the mixture temperature in the cylinder. The former temperature was measured at a position approximately 40 mm upstream of the scavenging port and the latter temperature was measured approximately 40 mm downstream of the exhaust port.

An internal EGR control valve (V_{in}) was installed in the exhaust pipe to apply internal EGR.

Throttling the flow through the internal EGR control valve lowered the scavenging ratio and applied internal EGR. The internal EGR rate was defined on the assumption that a state of complete mixing and scavenging existed in the cylinder. Assuming initial operating conditions of an engine speed N = 1000 rpm and WOT, the initial scavenging efficiency (η_{si}) and initial residual gas ratio (γ_i) were calculated from the scavenging ratio (SRi) at that time using the following equations (1)–(2).

$$\eta_{si}=1-\exp(-SR_i) \tag{1}$$

$$\gamma_i=1-\eta_{si}$$

The scavenging efficiency (η_s) and residual gas ratio (γ) were then calculated from the scavenging ratio (SR) when the flow through the internal EGR control valve was throttled.

$$\eta_s=1-\exp(-SR) \tag{2}$$

$$\gamma=1-\eta_s$$

Based on these calculations, the internal EGR rate (In-EGR) was defined as the difference between the residual gas ratio γ when the flow through the internal EGR control valve was throttled and the initial residual gas ratio γ_i. The In-EGR rate could be varied intentionally by adjusting the control valve setting and was given by following equation (3).

$$In\text{-}EGR=(\gamma-\gamma_i)\times 100\% \tag{3}$$

The characteristics used in analyzing the heat release waveforms are defined below and in Figure 3.

Maximum hot flame value Q_{Hmax}: maximum heat release rate of the hot flame

Ignition timing θ_{on}: the crank angle at which the heat release rate reaches 10% of Q_{Hmax}

Time of hot flame peak θ_{peak}: the crank angle at the time of the peak heat release rate of the hot flame

2.2. Calculation Method

Chemical kinetic simulations were performed using CHEMKIN software under dimensionless (i.e., spatially

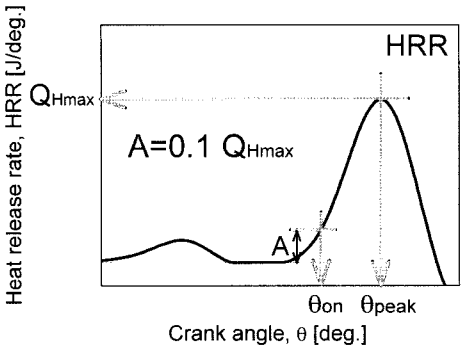

Figure 3. Definitions of characteristic values used in analyzing heat release rate waveforms.

uniform), adiabatic conditions and by applying the same volumetric changes as those of the test engine. The PRF reaction mechanisms (1034 chemical species, 4238 elementary reactions) developed at the Lawrence Livermore National Laboratory (Curran *et al.*, 1998a, 1998b, 2002) were used in the calculations.

Because internal EGR was applied under the ATAC condition, the composition and temperature of the gas were taken into account as noted below in setting the initial conditions of the calculations.

(1) EGR gas is composed of N_2, O_2, CO_2 and H_2O.

(2) The temperature at the onset of compression T_{epc} is given by the following equation, taking into account the temperature rise due to the residual gas (see Appendix).

$$T_{epc}=\eta_s T_{sc}+(1-\eta_s)T_r \quad (4)$$

where T_r and η_s denote the residual gas temperature and scavenging efficiency, respectively.

3. RESULTS AND DISCUSSION

3.1. Comparison of Ignition and Combustion Characteristics of HCCI and ATAC Processes

3.1.1. Influence of octane number on ignition characteristics

In order to compare the autoignition characteristics of HCCI combustion and ATAC, the relationship between the fuel octane number and ignition characteristics was investigated under the HCCI and ATAC operating conditions. Figures 4 and 5 show the heat release rate (HRR) waveforms obtained experimentally with test fuels of different octane numbers (RON) for HCCI combustion and ATAC, respectively.

In an octane number range of 0-60 RON, the scavenging temperature (T_{sc}) remained around 329–331 K in HCCI combustion. However, when either an 80 RON fuel or gasoline (91 RON) was used as the test fuel in HCCI combustion, the engine misfired and could not be operated stably. As a result, T_{sc} was raised to 360 K and 375 K, respectively, and the equivalence ratio was similarly increased to $\phi = 0.75$ and $\phi = 0.7$ in order to accomplish ignition. It is seen in Figure 5 that T_{sc} stayed in a range of 378–390 K under the ATAC conditions.

For the test fuels with octane numbers from 0 to 60 RON, the HRR waveforms for HCCI combustion in Figure 4 show a pattern of two-stage ignition resulting from the passage of a cool flame. Increasing the octane number had the effect of reducing the quantity of heat released by the cool flame (arrow A), and the ignition timing was delayed to a later crank angle (arrow B). In contrast to those results, all the HRR waveforms in

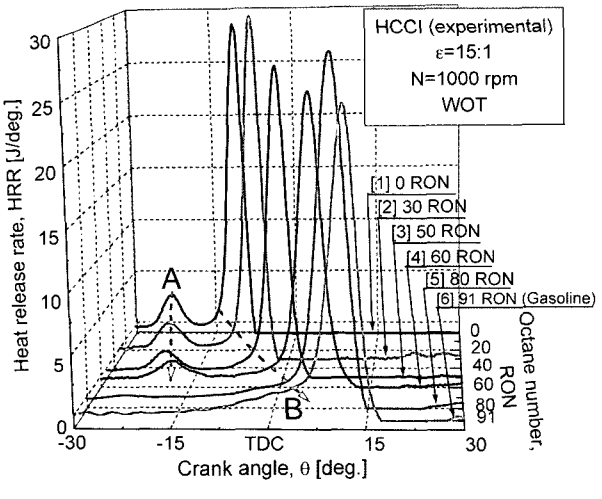

HCCI experimental			
	RON	ϕ [-]	Tsc [K]
1	0	0.5	329
2	30	0.5	330
3	50	0.5	331
4	60	0.5	329
5	80	0.75	360
6	91 (Gasoline)	0.7	375

Figure 4. Influence of octane number on HRR in HCCI combustion (experimental).

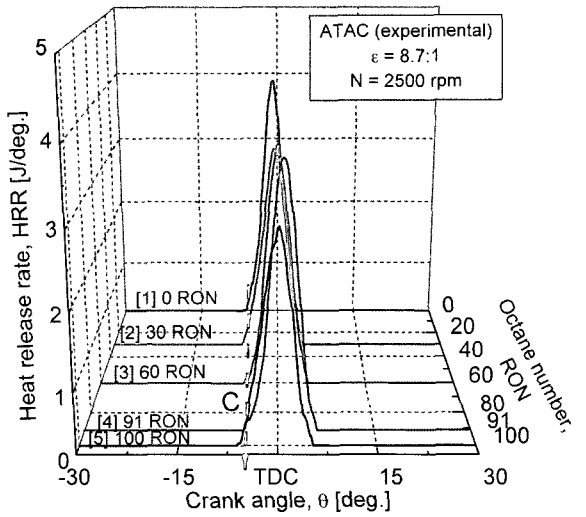

ATAC experimental				
	RON	ϕ [-]	Tsc [K]	ηs [-]
1	0	0.8	378	0.41
2	30	0.8	384	0.39
3	60	0.8	389	0.40
4	91 (Gasoline)	0.85	385	0.40
5	100	0.85	390	0.39

Figure 5. Influence of octane number on HRR in ATAC (experimental).

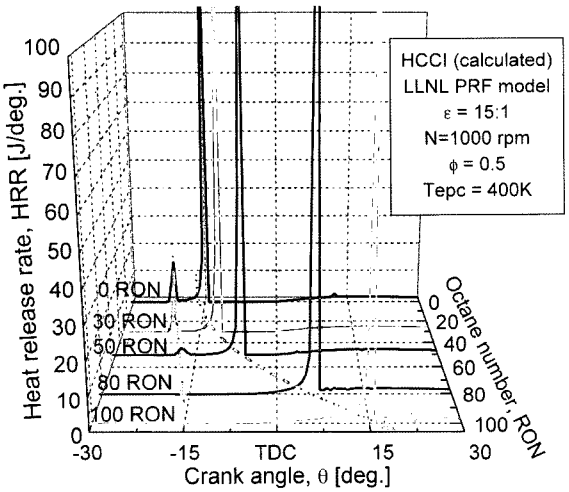

Initial gas composition	
Species	Mole fraction [%mole]
N2	79.00
O2	21.00
Total	100

Figure 6. Influence of octane number on HRR in HCCI (calculated).

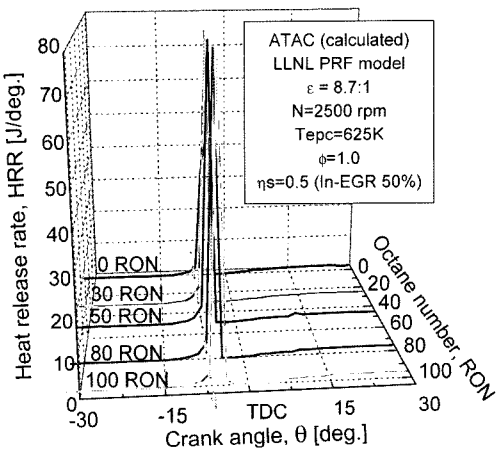

Initial gas composition	
Species	Mole fraction [%mole]
N2	77.28
O2	13.82
CO2	4.15
H2O	4.75
Total	100

Figure 7. Influence of octane number on HRR in ATAC (calculated).

Figure 5 for ATAC show a pattern of single-stage ignition without any passage of a cool flame. The ignition timing also remained virtually constant (arrow C) even when the octane number was increased. In other words, although the fuel octane number had a large effect on the ignition timing in HCCI operation, it had little effect under ATAC operation.

Next, we will present the numerical calculation results for HCCI combustion and ATAC. Figure 6 shows the HRR waveforms that were calculated under HCCI operating conditions for different fuel octane numbers, and Figure 7 shows the calculated HRR waveforms for ATAC operating conditions. The calculation conditions in both cases are shown in the box in the figure and in the table below the figure. As is evident in both figures, the calculated waveforms show nearly the same tendencies as the experimental data. It is clear that varying the fuel octane number had much less effect on the ignition timing in the ATAC process compared with HCCI combustion. It can be inferred from these results that fuels having a wide range of octane numbers can be autoignited in the ATAC process.

As the reason for that difference, we can consider the differences in the respective temperature histories followed by the ATAC and HCCI combustion processes. With HCCI combustion, increasing the fuel octane number retarded ignition, which presumably can be attributed to the low-temperature reaction rate stemming from the fuel's molecular structure (Pilling *et al.*, 1997), or in other words, the influence of a cool flame. In ATAC, a cool flame was not manifested even when a fuel with a low octane number was used, which is why little correlation is seen between the octane number and the change in ignition timing.

3.1.2. Comparison of autoignited reaction behavior

The foregoing results showed that the relationship between the fuel octane number and ignition timing differed greatly between HCCI combustion and ATAC. It was presumed that susceptibility to the occurrence of cool flame reactions was one reason for that difference. Accordingly, attention was focused on the results seen for the 0 RON fuel (n-heptane) in the experimental and calculated data presented for HCCI combustion and ATAC in Figures 4 to 7. A comparison was made of the behavior of the chemical species, such as the radicals, that were generated at the time cool flame reactions occurred.

3.1.2.1. Radical light emission behavior measured experimentally

Figures 8 and 9 show the details of typical waveforms measured experimentally for HCCI combustion and ATAC, respectively, using the 0 RON test fuel. From the top of each figure, the waveforms are for the cylinder pressure (P), HRR, light emission intensity of HCHO and the light emission intensity of the OH radical. It is observed in Figure 8 that the HRR waveform for HCCI combustion shows a pattern of two-stage ignition attributed to the manifestation of a cool flame and a hot flame. Simultane-

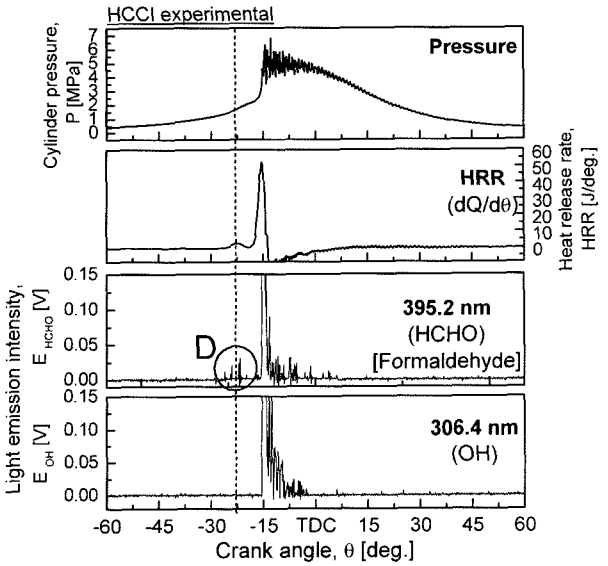

HCCI experimental				
ε [-]	N [rpm]	ϕ [-]	Throttle	Fuel (RON)
15:1	1000	0.6	WOT	n-heptane (0 RON)

Figure 8. Typical waveforms for HCCI combustion (experimental).

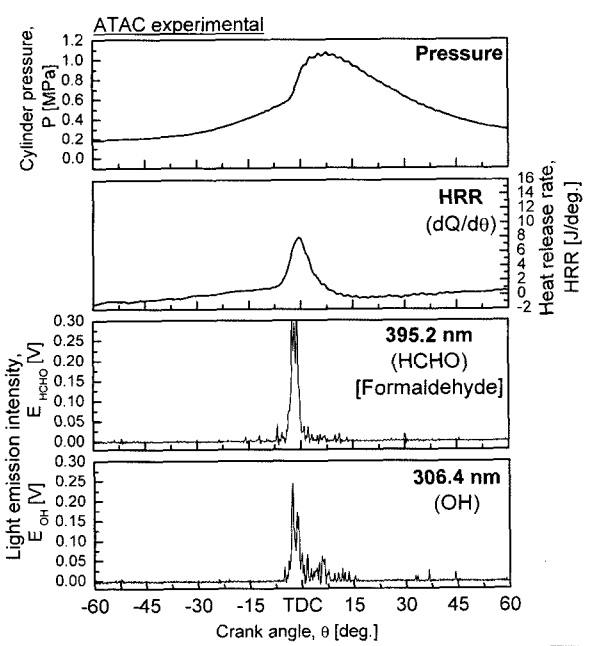

ATAC experimental					
ε [-]	N [rpm]	ϕ [-]	Throttle	SR [-]	Fuel (RON)
8.7 : 1	2500	1.0	Part throttle	0.5	n-heptane (0 RON)

Figure 9. Typical waveforms for ATAC (experimental).

ous with the passage of the cool flame, only the HCHO waveform shows evidence of faint light emission (region D). It is assumed that this faint light emission can be attributed to excited-state HCHO (Gaydon, 1957) and

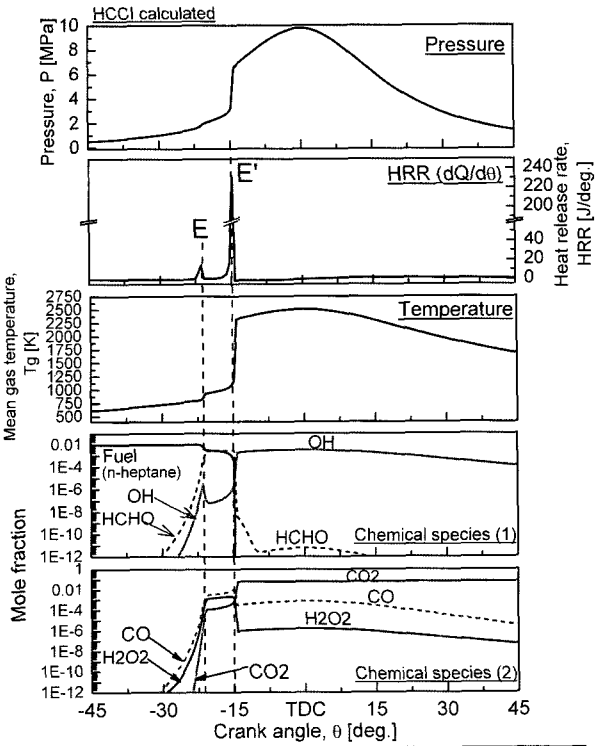

HCCI calculated					
ε [-]	N [rpm]	ϕ [-]	Throttle	Tepc [K]	Octane number
15:1	1000	0.6	WOT	400	0 RON (PRF 0)

Figure 10. Typical waveforms for HCCI combusion (calculated).

that it represents light emitted from the cool flame.

By contrast, the HRR waveform for ATAC in Figure 9 shows single-stage ignition attributed only to a hot flame and there is no evidence of the passage of a cool flame. Both the HCHO and OH radical waveforms only show signs of light emission simultaneous with the passage of the hot flame. These results for the light emission behavior of the radicals also indicate that the HCCI and ATAC processes differ in their susceptibility to the passage of a cool flame.

3.1.2.2. Behavior of chemical species based on chemical kinetic simulations

Figures 10 and 11 show the detailed calculated results for HCCI combustion and ATAC when using the 0 RON fuel. From the top of each figure, the waveforms show the cylinder pressure (P), HRR, mean in-cylinder gas temperature (T_g), and the mole fractions of chemical species (1) and (2). The latter waveforms are indicated on a logarithmic scale because the quantities of the chemical species produced during combustion differ greatly from one species to another.

Similar to the experimental results, the calculated HRR

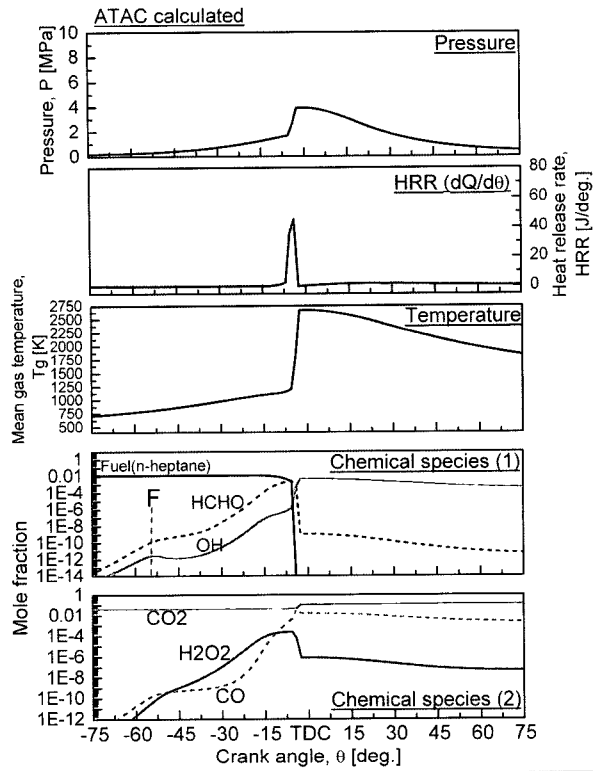

ATAC calculated					
ε [-]	N [rpm]	φ [-]	SR [-]	Tepc [K]	Octane number
8.7 : 1	2500	1.0	0.5	625	0 RON (PRF 0)

Figure 11. Typical waveforms for ATAC (calculated).

waveform for HCCI combustion in Figure 10 shows a pattern of two-stage ignition. Looking closely at the mole fraction behavior of the chemical specifies, it is seen that the mole fraction of HCHO and the OH radical increased sharply (line E) simultaneously with the consumption of fuel at the time a cool flame occurred. The quantity of HCHO produced increased in particular and was several hundred times greater than that of the OH radical. Subsequently, the quantity of OH radicals produced also increased simultaneously with the passage of a hot flame, while HCHO decreased sharply, and the quantity of CO_2 produced as the final combustion product increased. These results indicate that the chemical species produced in HCCI combustion also showed a pattern of two-stage behavior (lines E and E') with large differences corresponding to two-stage ignition.

On the other hand, the HRR waveform for ATAC in Figure 11 shows only single-stage ignition and no evidence of a cool flame. However, looking carefully at the mole fraction behavior of the chemical species, a small peak (line F) is seen in the vicinity of 55 deg. before top dead center (BTDC). It is assumed that this position corresponds to the occurrence of cool flame reactions. The level of the peak, however, is much lower than that seen for HCCI combustion. That is presumably the reason why no sign of a cool flame can be detected in the HRR waveform.

3.2. Influence of Internal EGR on HCCI Combustion at High Compression Ratio

The foregoing results indicated that a cool flame was not likely to occur in ATAC in the presence of a large quantity of residual gas (internal EGR) and also that the ignition timing tended not to vary in relation to the fuel octane number. One method that has attracted attention for inducing and controlling ignition in 4-stroke HCCI engines is to use negative valve overlap (NVO) or some other means to apply residual gas. In this regard, ignition and combustion characteristics were examined when internal EGR was applied under the HCCI conditions with a high compression ratio of $\varepsilon = 15{:}1$.

3.2.1. Influence of internal EGR on HRR waveforms

Figure 12 shows the HRR waveforms that were measured experimentally for various internal EGR rates under HCCI operation at a compression ratio of 15:1 and using the 0 RON test fuel. The quantity of fuel supplied (Q_{in}) was kept constant at 9.5±0.3 mg/cycle in all of the experiments in which these waveforms were measured. As seen in the figure, increasing the internal EGR rate advanced the passage of a cool flame to an earlier crank angle and decreased the quantity of heat released (arrow G). The ignition timing initially advanced as the internal EGR rate was increased, but it subsequently showed the opposite tendency and was delayed to a later crank angle (arrow H). It is inferred that the application of internal

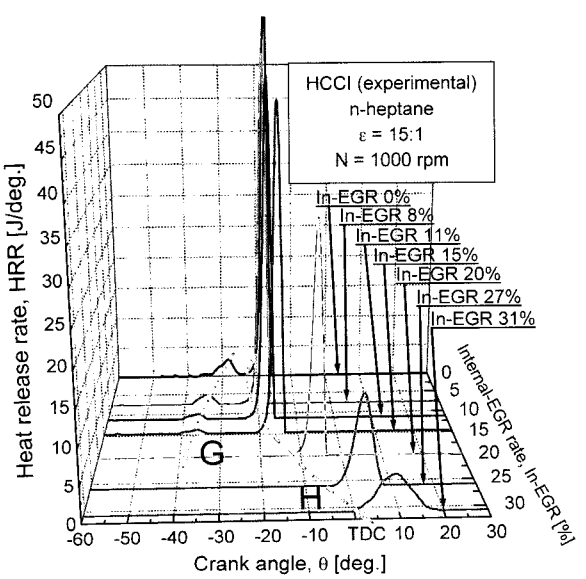

Figure 12. Influence of internal EGR on combustion.

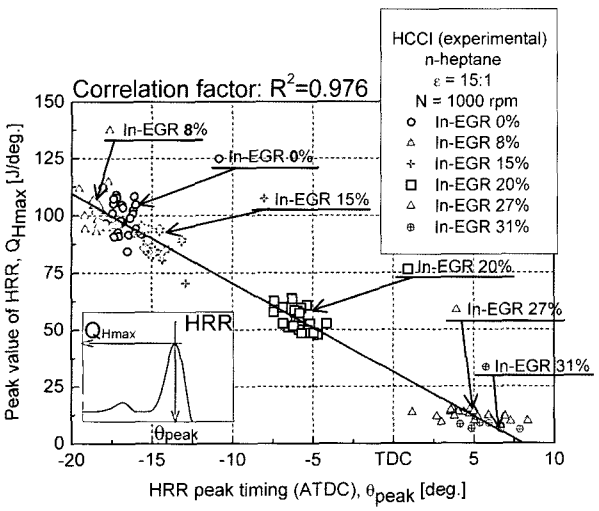

Figure 13. Peak heat release rate as a function of the crank angle (experimental).

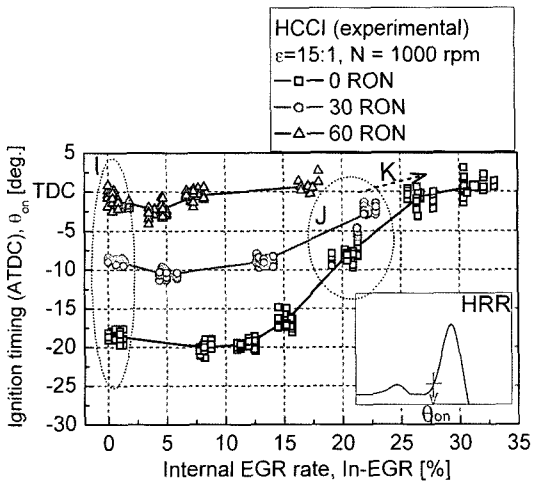

Figure 14. Ignition timing as a function of internal EGR rate for HCCI combustion of test fuels with different octane numbers.

EGR can either have the effect of advancing or retarding the ignition timing as explained in (i) to (iii) below, depending on the level applied.

(i) Heat contained in the internal EGR gas raises the temperature at the onset of compression, which has the effect of advancing the ignition timing.

(ii) Because it lowers the specific heat ratio, it has the effect of retarding the ignition timing.

(iii) Because it reduces the quantity of heat released by a cool flame, it has the effect of retarding the ignition timing.

The interaction of these factors is thought to account for the reversal of the ignition timing from an earlier to a later crank angle.

It is also seen that the peak value of the HRR waveforms decreased and that the combustion rate was moderated as the internal EGR rate was increased (Figure 12). One reason for that is presumed to be the retarding of the ignition timing. Another reason is that the inert gases in EGR had the effect of slowing down combustion. In the experiments conducted in this study, the fuel injection quantity was kept constant at all of the internal EGR rates used. For that reason, the peak value of the HRR waveform can be regarded as representing the rate of combustion reactions. Accordingly, an investigation was made of the relationship between the peak HRR (Q_{Hmax}) and the crank angle (θ_{peak}), and the results are shown in Figure 13. As the results in the figure indicate, there was a strong correlation between the two, and retarding the ignition timing was effective in moderating the rate of combustion.

3.2.2. Combined influence of fuel octane number and internal EGR on ignition characteristics

The preceding discussion revealed that the ignition characteristics of HCCI combustion and ATAC differed considerably in relation to the fuel octane number. That difference is attributed to the different degrees of susceptibility of these combustion processes to the occurrence of cool flame reactions, depending on the level of internal EGR applied.

Figure 14 shows the ignition timing (θ_{on}) found for test fuels with different octane numbers when internal EGR was applied under the HCCI operating conditions (compression ratio of 15:1 and WOT). The results indicate that the ignition timing was retarded in the region of a low internal EGR rate as the fuel octane number was increased (region I). However, as the internal EGR rate was increased, the difference in ignition timing between the different fuel octane numbers decreased (region J and arrow K). These results reveal that the application of internal EGR to the 4-stroke HCCI combustion process at a high compression ratio results in the same ignition characteristics as those of 2-stroke HCCI combustion (ATAC) at part throttle. It was reported that the ignition timing showed little change in relation to changes in the fuel octane number under 4-stroke HCCI operation when residual gas was applied (Risberg *et al.*, 2004) by means of NVO. Presumably, the state of combustion in that study was similar to the present results.

It is inferred from the foregoing results that, under high-compression-ratio HCCI operation as well, the ignition timing is less likely to be influenced by changes in the fuel octane number when the internal EGR rate is increased. Under the application of heavy internal EGR in particular, it is thought that the range in which the ignition timing can be varied by changing the fuel composition (i.e., octane number) becomes smaller compared

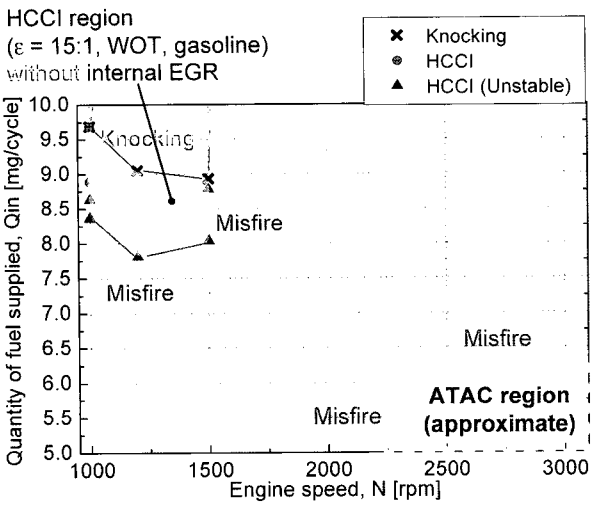

Figure 15. Region of stable engine operation for HCCI combustion without internal EGR (Test fuel = gasoline; experimental).

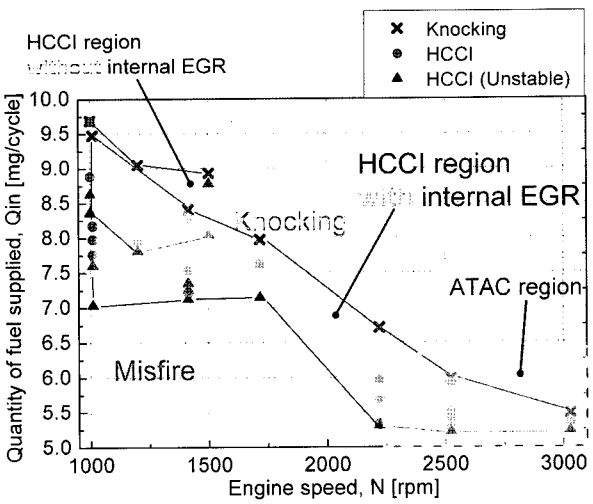

Figure 16. Region of stable engine operation for HCCI combustion with EGR (Test fuel = gasoline; experimental).

with that for non-EGR operation.

3.2.3 Influence of internal EGR on the engine operation region under high-compression-ratio HCCI combustion Figure 15 shows the region in which the test engine could be operated stably on gasoline (91 RON) under the high-compression-ratio HCCI conditions (ε= 15:1) without the application of internal EGR. The engine load is expressed by the engine speed shown along the horizontal axis and the quantity of fuel supplied per cycle shown along the vertical axis. The test engine could not be operated in the region above the "x" marks on account of knocking, nor in the region below the solid triangles (▲) because of misfiring. The area in between represents the region in which operation was possible under HCCI combustion. The approximate region in which engine operation was possible under ATAC is also shown for comparison.

As the results in the figure indicate, engine operation became impossible under these HCCI conditions in the vicinity of an engine speed of N = 1500 rpm owing to the occurrence of misfiring. By contrast, engine operation was possible under the ATAC conditions (ε= 8.7:1) at engine speeds above approximately 2200 rpm. It will be noted that experiments were not conducted at engine speeds above 3000 rpm on account of the allowable speed limit of the dynamometer used in this study. One characteristic of ATAC suggested by these results is that stable engine operation is possible at rather high engine speeds. In fact, it has been reported that engine operation in the high-speed range above 8000 rpm is possible under AR combustion (Ishibashi *et al.*, 1996), which is a combustion process similar to ATAC. The experimental data presented here indicate that the engine speed range allowing stable operation tends to be the exact opposite between high-compression-ratio HCCI combustion and ATAC.

Figure 16 shows the change in the region of stable operation when the internal EGR control valve was partially closed to change the operating parameters from the HCCI conditions to the application of an internal EGR rate of approximately 12%. As seen in the figure, the application of internal EGR expanded the operation region on the high-speed, low-load side, bringing it close to the operation region for ATAC. This indicates that the application of internal EGR to high-compression-ratio HCCI combustion can result in a region of stable engine operation close to that attained with ATAC.

4. CONCLUSIONS

In this study, HCCI combustion in a 4-stroke engine was simulated by operating a 2-stroke engine at a higher compression ratio (ε= 15:1), making it possible to use the same test engine to compare the combustion characteristics with those of the 2-stroke HCCI (ATAC) process under ordinary operating conditions. Additionally, the influence of internal EGR and different fuel compositions (octane numbers) on ignition and combustion characteristics was investigated under conditions that simulated HCCI combustion in a 4-stroke engine. The following results were obtained.

Comparison of HCCI combustion and ATAC

(1) One significant difference between HCCI combustion and ATAC was shown to be their different degrees of susceptibility to the occurrence of cool flame reactions. It was found that ATAC was much less suscep-

tible to cool flame reactions than HCCI combustion.

(2) The ignition timing did not change appreciably in ATAC when test fuels of different octane numbers (RON) were used. This indicates that the ignition timing in this combustion process has low sensitivity to changes in the fuel octane number.

(3) In HCCI combustion, the quantity of heat released by a cool flame decreased as the fuel octane number was raised, with the result that the ignition timing was retarded to a later crank angle. This suggests that the ignition timing in HCCI combustion is highly sensitive to changes in the octane number.

Influence of internal EGR on high-compression-ratio HCCI combustion

(4) It was found that internal EGR had the dual effects of advancing or retarding the ignition timing.

(5) The application of internal EGR to high-compression-ratio HCCI combustion produced a combustion state resembling ATAC. Specifically, the quantity of heat released by a cool flame was reduced and before long the flame was extinguished. Under the application of internal EGR the ignition timing tended not to change in relation to different fuel octane numbers.

(6) Applying internal EGR to the conditions of high-compression-ratio HCCI combustion tended to expand the region of stable engine operation on the low-load, high-speed side, bringing it closer to the operation region for ATAC.

REFERENCES

Aoyama, T., Hattori, Y., Mizuta, J. and Sato, Y. (1996). An experimental study on premixed-charge compression-ignition gasoline engine. *SAE Paper No.* 960081.

Blair, G. (1996). *Design and Simulation of Two-Stroke Engines*. Society of Automotive Engineers, Inc., USA.

Choi, G. H., Han, S. B. and Dibble, R. W. (2005). Experimental study on homogeneous charge compression ignition engine operation with exhaust gas recirculation. *Int. J. Automotive Technology* **5, 3**, 195–200.

Curran, H. J., Gaffuri, P., Pitz, W. J. and Westbrook, C. K. (1996). A Comprehensive modeling study of n-heptane oxidation. *Combustion and Flame*, **114**, 149–177.

Curran, H. J., Pitz, W. J., Westbrook, C. K., Callahan, C. V. and Dryer, F. L. (1998). Oxidation of automotive primary reference fuels at elevated pressures. *Proc. Combust. Inst.*, **27**, 379–387.

Curran, H. J., Gaffuri, P., Pitz, W. J. and Westbrook, C. K. (2002). A comprehensive modeling study of iso-octane oxidation. *Combustion and Flame,* **129,** 253–280.

Gaydon, A. G. (1957). *The Spectroscopy of Flame.* Chapman and Hall Ltd.. London.

Ishibashi, Y. and Asai, M. (1996). Iroving the ehaust eissions of two-stroke engines by applying the activated radical combustion. *SAE Paper No.* 960742.

Lavy, J., Dabadie, J.-C., Angelberger, C., Duret, P., Willand, J., Juretzka, A., Schäflein, J., Ma, T., Lendresse, Y., Satre, A., Schulz, C., Krälmer, H., Zhao, H. and Damiano, L. (2000). Innovative ultra-low NOx controlled auto-ignition combustion process for gasoline engines: The 4-space project. *SAE Paper No.* 2000-01-1837.

Lee, K. H. Gopalakrishnan, V. and Abraham, J. (2004). An investigation of the effect of changes in engine operating conditions on ignition in an HCCI engine. *J. Mechanical Science and Technology* **18, 10**, 1809–1818.

Onishi, S., Jo, S. H., Shoda, K., Jo, D. P. and Kato, S. (1979). Active thermo-atmosphere combustion (ATAC) –A new combustion process for internal combustion engines. *SAE Paper No.* 790501.

Pilling, M. J. (Editor) (1997). *Low-Temperature Combustion and Autoignition.* Comprehensive Chemical Kinetics, **35**. Elsevier. Amsterdam.

Risberg, P., Kalghatgi, G. and Angstrom, H. (2004). The influence of EGR on autoignition quality of gasoline-like fuels in HCCI engines. *SAE Paper No.* 2004-01-2952.

Sato, S., Kweon, S. P., Yamashita, D. and Iida, N. (2006). Influence of the mixing ratio of double componential fuels on HCCI combustion. *Int. J. Automotive Technology* **7, 3,** 251–259.

Shoji, H., Amino, Y., Hashimoto, S., Yoshida, K. and Saima, A. (1998). Clarification of OH radical emission intensity during autoignition in a 2-stroke spark ignition engine. *SAE Paper No.* 982481.

Thring, R. H. (1989). Homogeneous charge compression-ignition (HCCI) engines. *SAE Paper No.* 892068.

Urushihara, T., Hiraya, K., Kakuhou, A. and Itoh, T. (2003). Expansion of HCCI operating region by the combination of direct fuel injection, negative valve overlap and internal fuel reformation. *SAE Paper No.* 2003-01-0749.

APPENDIX

Estimation of In-Cylinder Gas Temperature at the Onset of Compression (Temperature at Exhaust Port Closing)

In this study, the in-cylinder gas temperature at the onset of compression (T_{epc}) was defined as shown below as the initial condition of the calculations when internal EGR was applied.

Definition (1) T_{epc} is defined as the temperature of the mixture of new air and residual gas.

Letting η_s denote the scavenging efficiency, T_{sc} the new air temperature (scavenging temperature) and Tr the

residual gas temperature, T_{epc} can be given by the following equation.

$$T_{epc}=\eta_s T_{sc}+(1-\eta_s)T_r \quad \text{[A-1]}$$

The scavenging efficiency (η_s) is calculated on the basis of scavenging ratio (SR), assuming perfect mixing scavenging (Blair, 1996).

$$\eta_s=1-e^{-SR} \quad \text{[A-2]}$$

Definition (2) Tr is defined as the average value of the blow-down temperature (T_{epo}), calculated from the peak cylinder pressure (P_{max}), and the measured exhaust temperature (T_{ex}).

$$T_{epo}=T_{\max}\left(\frac{P_{epo}}{P_{\max}}\right)^{\frac{n-1}{n}}$$

$$T_r=\frac{T_{epo}+T_{ex}}{2}=\frac{T_{\max}(P_{epo}/P_{\max})^{\frac{n-1}{n}}+T_{ex}}{2} \quad \text{[A-3]}$$

From Equations. [A-1], [A-2] and [A-3], T_{epc} can be calculated with the following equation [A-4].

$$T_{epc}=(1-e^{-SR})T_{sc}+e^{-SR}\frac{T_{\max}(P_{epo}/P_{\max})^{\frac{n-1}{n}}+T_{ex}}{2} \quad \text{[A-4]}$$